Characterization of Thin Electroless Nickel Coatings

Nicholas M. Martyak

Atotech USA, Inc., Somerset, New Jersey 08875

Received March 2, 1994. Revised Manuscript Received June 20, 1994[⊗]

The early stages of electroless nickel growth on copper {100} were characterized using scanning tunneling and transmission electron microscopy. A long induction time was observed prior to nickel deposition. Scanning tunneling microscopy analysis showed all deposits grew by the lateral spreading of atomic layers followed by the formation and coalescence of three-dimensional structures. Transmission electron microscopy studies showed low-phosphorus electroless nickel coatings consisted of discrete islands which coalesced into continuous films. Low-phosphorus deposits were crystalline. Medium-phosphorus deposits were more continuous than low phosphorus coatings and exhibited a semiamorphous structure. High-phosphorus deposits were continuous and amorphous. This size of coherently diffracting crystallites decreased with an increase in the phosphorus content of the nickel films. Three dimensional surface structures observed with STM agrees with the size of the crystallites from TEM analysis.

Introduction

The growth of deposited films, both vapor and electrodeposited ones, can occur on substrates by one of three mechanisms.[1] Volmer–Weber growth occurs if the surface energy of the deposited film is greater than that of the substrate. This mode of growth is characterized by three-dimensional crystallites developing directly on the substrate. If the surface energy of the film is low compared to that of the substrate, Frank–van der Merwe or layer growth dominates. Stranski–Krastanov growth consists of thin-layer formation in which the three-dimensional crystallites then grow. When the strain energy in the film is small, Frank–Van der Merwe growth occurs, whereas if the strain in the deposited film is large, the Stranski–Krastanov mechanism predominates. Layer growth is usually associated with epitaxy between the deposit and the substrate.

Epitaxial deposition can occur by the lateral spreading of layers of atoms.[2,3] There is evidence that very thin layers of copper or gold on nickel and nickel or gold on copper spread over the substrate as monolayers. Krakow and Hines[4] reported that gold forms large three-dimensional crystallites after the deposit is 0.9 nm thick. Jesser and Matthews[5] showed cobalt was deposited on a copper single crystal as monolayers up to a thickness of 2.0 nm. Layer growth has been observed for gold deposits on silver[6] as well as for nickel deposits on copper substrates[4]

The extent of epitaxial-layer formation may depend on several variables. Royer[7] stated the misfit between the two layers must be less than 15% for epitaxy. However, Pashley[8] claimed that the degree of misfit did not determine the extent of epitaxial growth. Bauer[9] found the interfacial energy between the coating and the substrate influenced the degree of epitaxy. Green et al.[10] showed that surface energies are more important in determining the extent of epitaxial growth than the misfit. Itoh et al.[11] studied the morphological changes in various metal deposits on copper single crystals. Differences in nucleation and growth behavior were

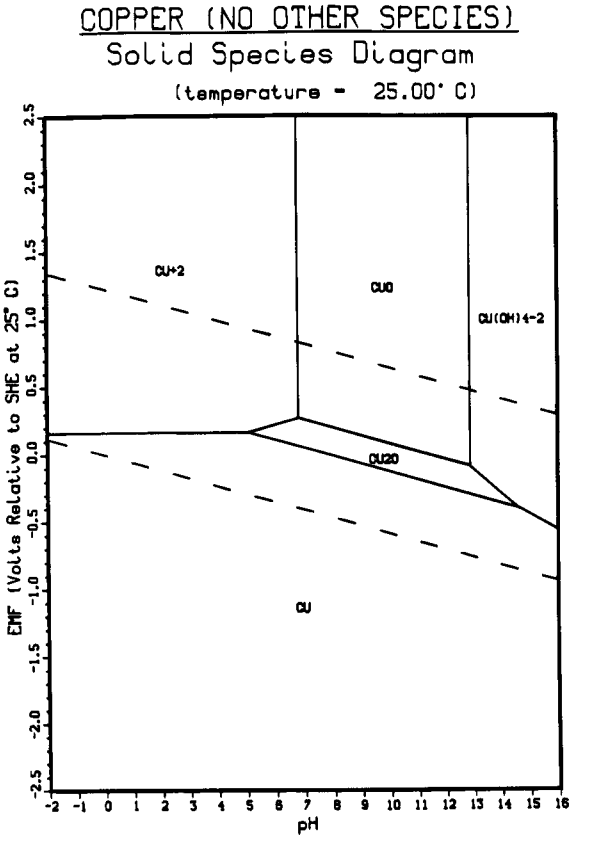

Figure 1. Potential–pH diagram for copper.

[⊗] Abstract published in *Advance ACS Abstracts,* August 15, 1994.

(1) Bauer, E.; Poppa, H. *Thin Solid Films* **1972,** *12,* 167.
(2) Lawless, K. R. *J. Vac. Sci Technol.* **1965,** *2,* 24.
(3) Thompson, E. R.; Lawless, K. R. *Electrochim. Acta* **1969,** *14,* 269.
(4) Krakow, W.; Hines, R. L. *J. Appl. Phys.,* **1971,** *42,* 3284.
(5) Jesser, W. A.; Matthews, J. W. *Philos. Mag.* **1968,** *17,* 461.
(6) Rao, S. T.; Weil, R. *J. Electrochem. Soc.* **1980,** *127,* 1030.
(7) Royer, L. *Bull. Soc. Fr. Mineral Crist.* **1928,** *51,* 7.
(8) Pashley, D. W. *Adv. Phys.* **1956,** *5,* 173.
(9) Bauer, E. *Z. Kristallogr.* **1958,** *110,* 395.
(10) Green, A. K.; Dancy, J.; Bauer, E. *J. Vac. Sci. Technol.* **1969,** *7,* 159.
(11) Itoh, S.; Yamozoe, N.; Seiyama, T. *Surf. Technol.* **1977,** *5,* 27.

0897-4756/94/2806-1667$04.50/0

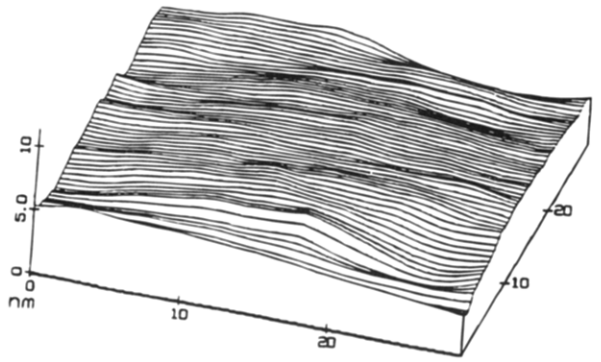

Figure 2. STM of copper substrate after electropolishing.

related to surface diffusion and exchange current densities. Itoh determined that epitaxial growth was related to directional coincidence of the most densely packed atomic rows of the substrate and the deposit. Impurities on the substrate surface can have a more important influence on epitaxy than the lattice misfit.[10]

Epitaxial growth may also occur[12,13] by the formation and subsequent coalescence of three-dimensional, epitaxial crystallites (TEC). The crystallites develop because of bunching which is due in part to growth impeding substances (basic colloidal compounds or addition agents) which stop lateral growth.[14] New layers spread laterally only as far as the one beneath. Rao and Weil[14] found evidence of TEC formation due to impurities in the plating solution. The formation of TEC may also be due to the misfit strain between the substrate and the coating.[12] The degree of such epitaxial growth is also affected by other factors. Epitaxy is favored on clean metallic surfaces free of oxides and surfaces that are not plastically deformed. Epitaxy is also favored when the current density is not too great, so as to allow atoms arriving on the surface of the deposit to diffuse and become incorporated into suitable kink sites. Two and three-dimensional nucleation has been observed[15-17] when kink sites are blocked or not formed at a fast enough rate so as to keep up with incoming metal atoms. Such would be the case when the current density is high. Three-dimensional nucleation has also been observed when the surface was covered by oxides or scale.[18,19]

This study was undertaken to characterize the structure of thin electroless nickel deposits on copper{100}. In particular, the initiation of EN deposition was monitored because copper does not readily oxidize hypophosphite. The early stage of electroless nickel growth was studied using transmission electron and scanning tunneling microscopy to gain insight into the third dimension of transmission electron micrographs. The effect of varying the percent phosphorus, through changes in solution chemistry, in the coatings on deposit structure was also investigated.

Experimental Section

Cubed-textured copper foil with a predominant {100} orientation was cut to approximately 10.0 × 10.0 cm and masked off with stop-off material exposing a square of about 100 cm^2.

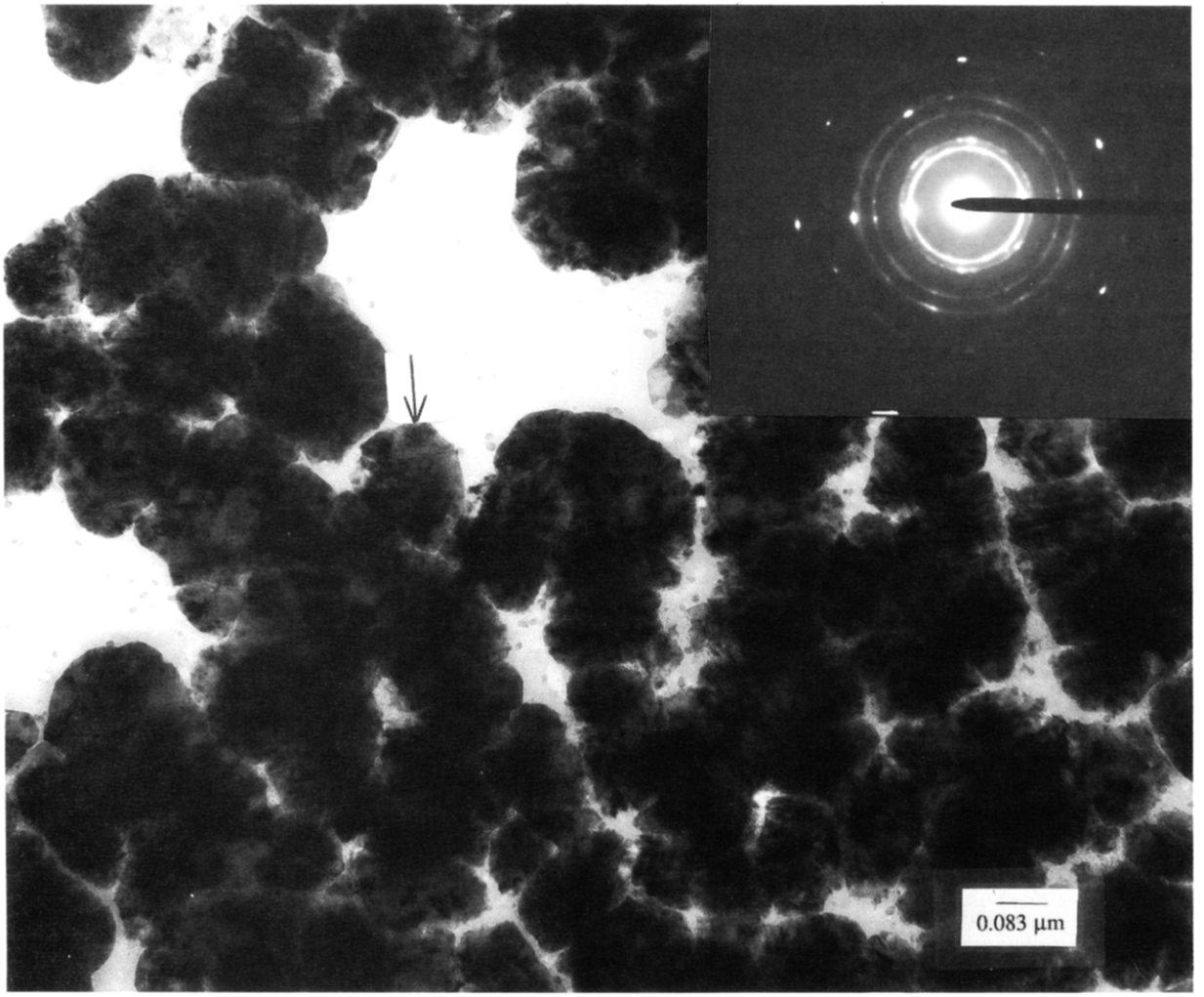

Figure 3. Bright-field TEM of low-phosphorus EN coating.

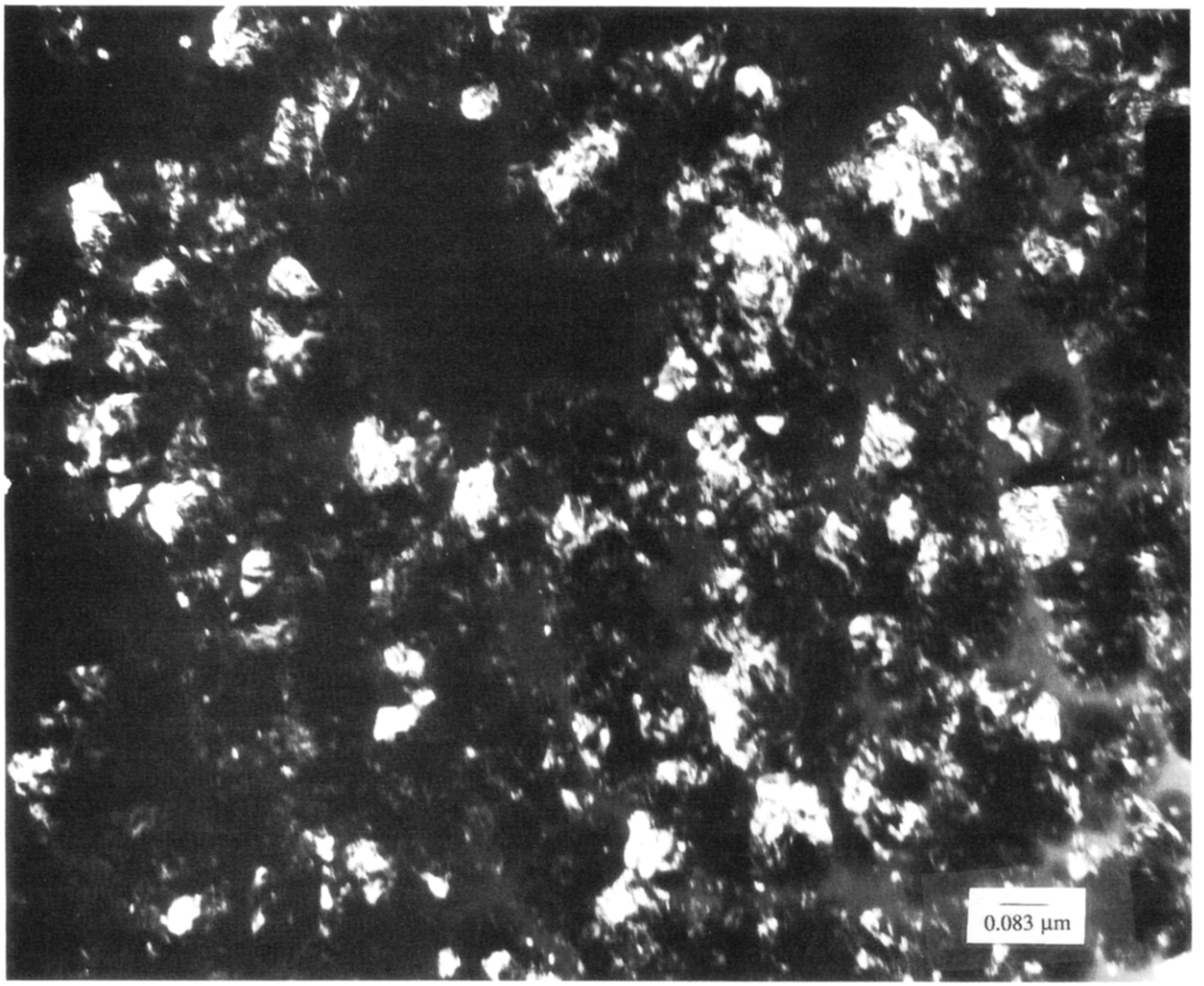

Figure 4. Dark-field TEM of low-phosphorus EN coating.

The copper was electropolished in 67% H_3PO_4 at 1.7 V for 3 min. The sample was rinsed in 10% H_3PO_4 followed by two water rinses.

The composition of the low phosphorus electroless nickel solutions contained 30 g/L $NiSO_4$, 15 g/L $H_2PO_2^-$, 30 mL/L lactic acid, 10 mL/L acetic acid, 5 mL/L propionic acid, and 10 g/L 2-hydroxyethanesulfonic acid,[20] pH 6.9. The medium-phosphorus electroless nickel solutions contained 30 g/L $NiSO_4$, 15 g/L $H_2PO_2^-$, 40 mL/L lactic acid, 15 mL/L acetic acid, 10 mL/L propionic acid, and 10 g/L 2-hydroxyethanesulfonic acid, pH 4.8. The high phosphorus electroless nickel solutions contained 20 g/L $NiSO_4$, 15 g/L $H_2PO_2^-$, 40 mL/L lactic acid, 15 mL/L acetic acid, 10 mL/L propionic acid, 20 g/L tartaric acid, and 0.5 ppm thiourea, pH 4.8.[21] All solutions were operated at 90 °C.

Chromium was deposited on the copper {100} surface from a solution containing 250 g/L CrO_3 and 2.5 g/L H_2SO_4. This chromium solution was operated at 55 °C and 0.5 mA/cm^2. The chromium thickness was 50 nm.

The surface structures of the electroless nickel and chromium deposits (all deposits 50 nm thick) were examined by scanning tunneling microscopy (STM). Sections of the elec-

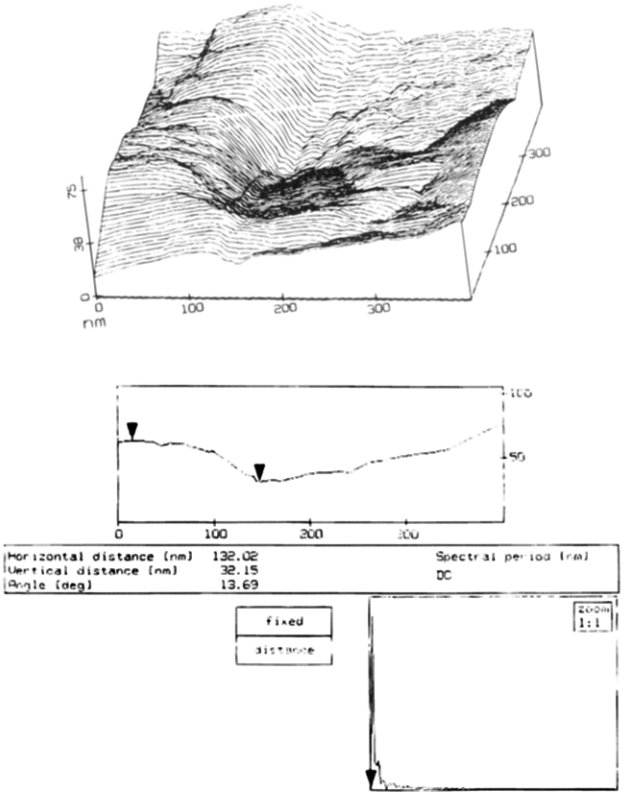

Figure 5. STM of low-phosphorus EN deposit showing crevice.

(12) Nakhara, S. *Thin Solid Films* **1980**, *61*, 241.
(13) Gaigher, H. L.; Van Wyk, G. N. *Electrochim. Acta* **1973**, *18*, 849.
(14) Rao, S. T.; Weil, R. *Trans. Inst. Met. Finish.* **1979**, *57*, 97.
(15) Weil, R. *Ann. Rev. Mater. Sci.* **1989**, 165.
(16) Felder, E. C.; Nakahara, S.; Weil, R. *Thin Solid Films* **1981**, *84*, 197.
(17) Weil, R. *Plat. Surf. Finish.* **1982**, *69*, 46.
(18) Kim, W.; Weil, R. *Trans. Inst. Met. Finish.* **1987**, *31*, 143.
(19) Feigenbaum, H.; Weil, R. *Surf. Coating Technol.* **1979**, *5*, 27.
(20) Martyak, N. M.; Monkyk, B. F.; Chien, H. H. US Patent 5,228,061, 1993.
(21) Martyak, N. M.; Monkyk, B. F., US Patent 5,306,334, 1994.

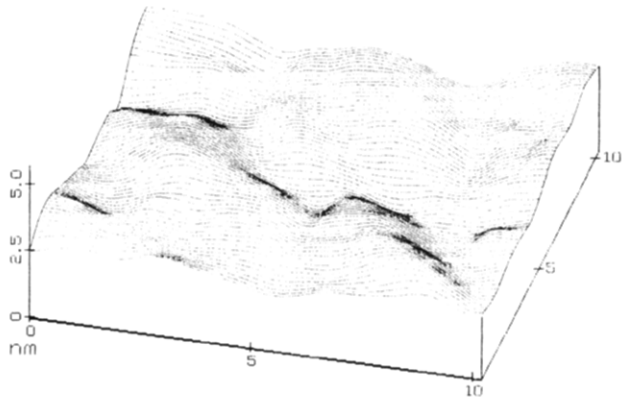

Figure 6. STM of low-phosphorus EN deposit showing TDS.

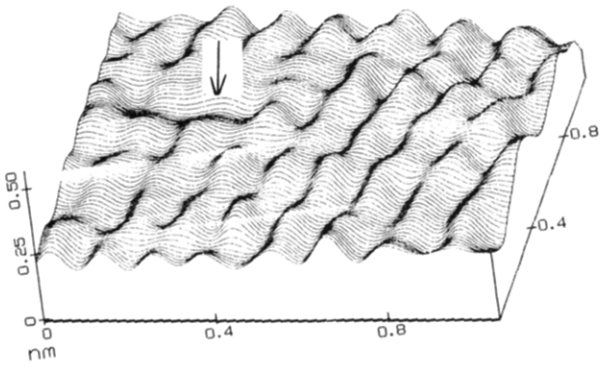

Figure 7. STM of low-phosphorus coating showing {220} planes.

troless nickel films attached to TEM grids were placed on the stage of the STM cell. Two different scanning heads, 1.0 μm and a 12 μm, were used. Various scanning speeds were employed. Platinum–iridium tips were used for atomic-scale imaging. The structures of thin EN films were also studied using transmission electron microscopy (TEM). Electroless nickel films approximately 50 nm thick were deposited on the copper substrate. The substrates were masked using stop-off material so as to expose a 3 cm^2 area. After plating, the masking material was removed in acetone. The copper substrates were then dissolved by floating the sample on a solution containing 500 g/L CrO_3 and 50 mL/L H_2SO_4 at room temperature. The electroless nickel foils and the chromium foil were than rinsed several times in distilled water, mounted on copper grids, and dried with methanol.

Results

The incubation time for EN deposition varied with the solution. For low phosphorus solutions, EN on the copper substrate occurred after 6 h. For the medium- and high-phosphorus solutions, deposition occurred after 5 and 4.5 h, respectively. In all three solutions, metallic nickel was seen depositing on the sides of the beakers indicating some solution instability. The potential–pH diagram for copper in the absence of any chelating agent is shown in Figure 1. The open-circuit potential for copper in the electroless nickel solutions listed above is approximately −0.295 V vs SCE. The potential changes slightly in the different solutions, but the copper electrode remains close to the Cu_2O domain in the low-phosphorus solutions and in the Cu domain in the medium- and high-phosphorus solution.

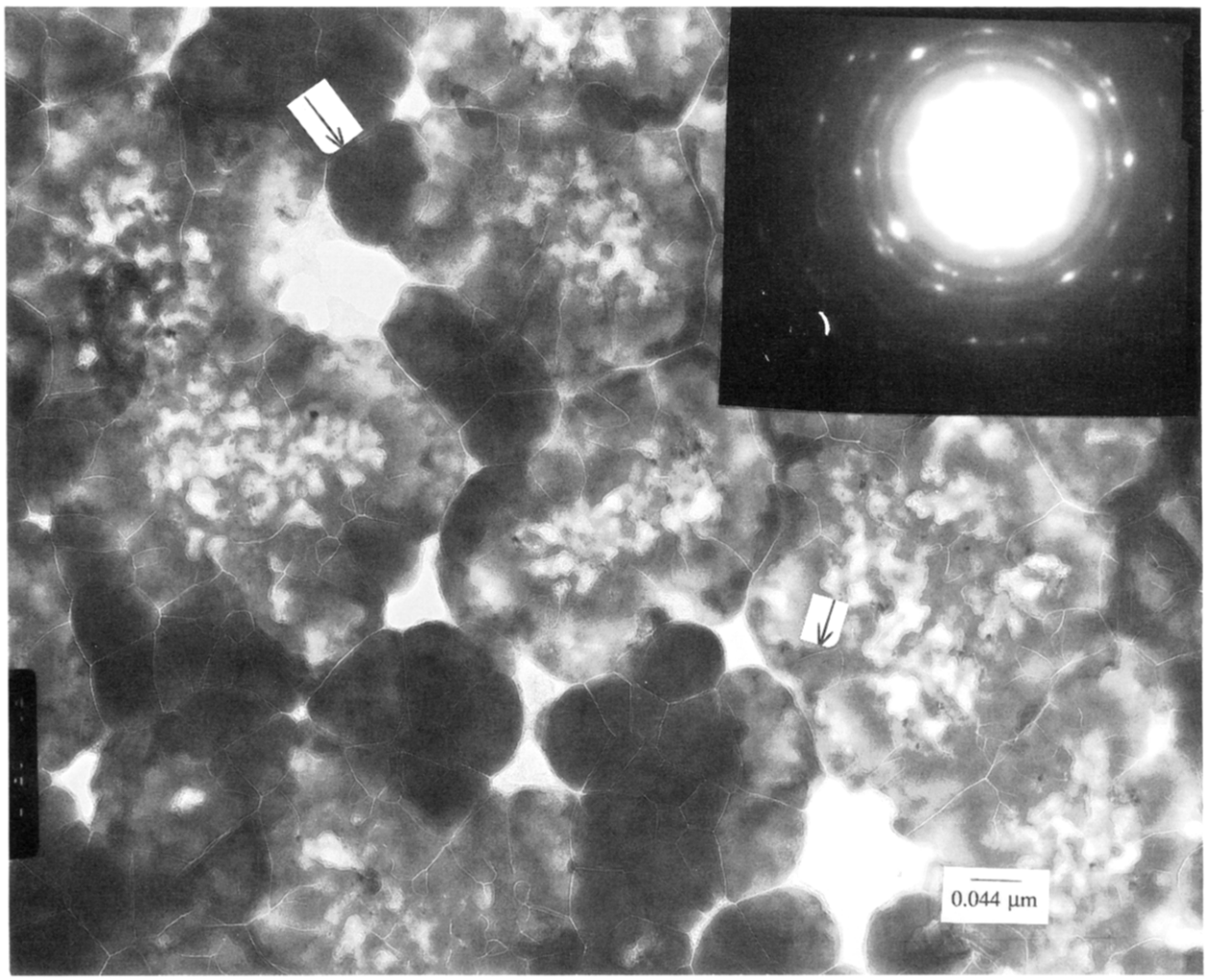

Figure 8. Bright-field TEM of medium-phosphorus EN coating.

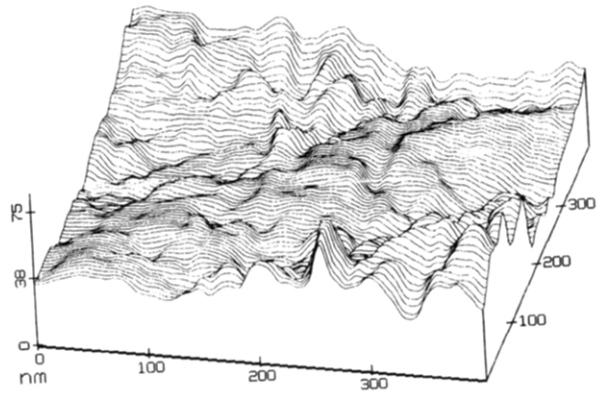

Figure 9. STM of medium-phosphorus EN deposit.

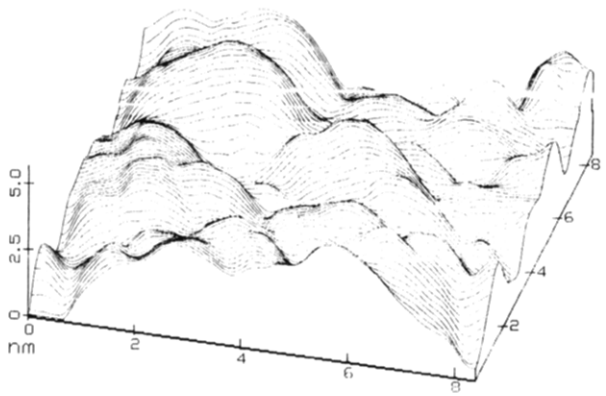

Figure 10. STM of medium-phosphorus EN deposit showing TDS.

An STM image of the copper substrate after electropolishing is shown in Figure 2. There are small surface undulations approximately 10 nm across and 2−5 nm high.

Transmission electron microscopy studies of low-phosphorus coatings shows the initial stages of growth were islands (Figure 3), which coalesced into a continuous layer with increasing deposit thickness. The size of the islands is approximately 200 nm. There is fine structure within each of the islands as well as between the islands as indicated by the arrow in Figure 3. Electron diffraction shown in the upper corner of Figure 3 reveals these films are crystalline. Dark field images (Figure 4), shows the size of the coherently diffracting domains is approximately 5 nm. The larger white areas in Figure 4 are groups of fine grains which satisfy the Bragg criterion.

Scanning tunneling microscopy of low phosphorus EN deposits shown in Figures 5−7 reveals the third dimension of the TEM images. Figure 5 shows relatively large structures approximately 100 nm across and 100−200 nm in length. This is approximately the same size of the individual islands in Figure 3. Surrounding these large structures are crevices. The sectional plot (Figure 5) shows these crevices are approximately 30−50 nm deep. Figure 6 shows smaller three dimensional features about 3−7 nm across and 3 nm in height. These features are the same size as the coherently diffracting crystallites measured in the TEM studies. Figure 7 shows a series of individual atoms transversing the image from the bottom left to the top right. The distance between the rows of atoms is 0.13 nm. A surface vacancy in the {220} planes of nickel is indicated by the arrow in Figure 7.

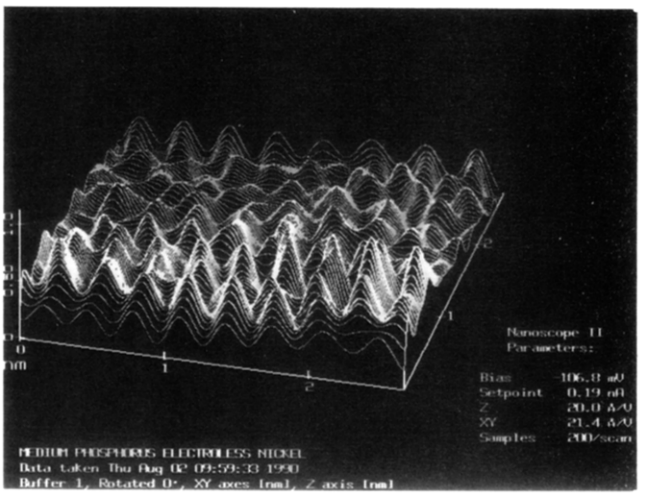

Figure 11. STM of medium-phosphorus coating showing individual nickel atoms.

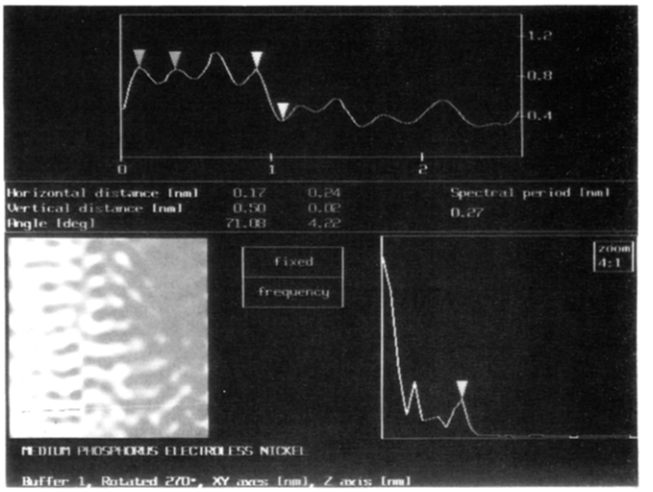

Figure 12. STM line trace of medium-phosphorus deposit revealing an atomic step.

Medium phosphorus deposits shown in Figure 8 are more continuous than the low-phosphorus coatings. The size of the largest individual domains indicated by the arrow in Figure 8 is about 70 nm. The larger areas indicated by the upper arrow in Figure 8 have less well defined boundaries. The fine structure observed within and between the islands in Figure 8 is less well defined than in Figure 3. Electron diffraction analysis indicates a semiamorphous structure, diffractions spots superimposed on an amorphous halo.

STM analysis shown in Figure 9 reveals a smoother surface than the low-phosphorus deposits. The large surface depressions observed in Figure 5 are not present in the medium-phosphorus films. Three-dimensional surface features approximately 20 nm across and 10 nm high are apparent. Figure 10 shows a high-magnification image of Figure 9. Three-dimensional crystallites about 2−5 nm are seen. Figure 11 is a three-dimensional image of a side of a three-dimensional surface structure (TDS) from Figure 10 showing individual nickel atoms. A sectional plot (Figure 12) shows a line trace across a section of the atoms is 0.24 nm. Also observed is an atomic step where the distance between the top and the bottom of the step is 0.5 nm.

High-phosphorus EN deposits shown in Figure 13 exhibit no well defined structure. There appears to be steps on the order of 35 nm. Electron diffraction showed

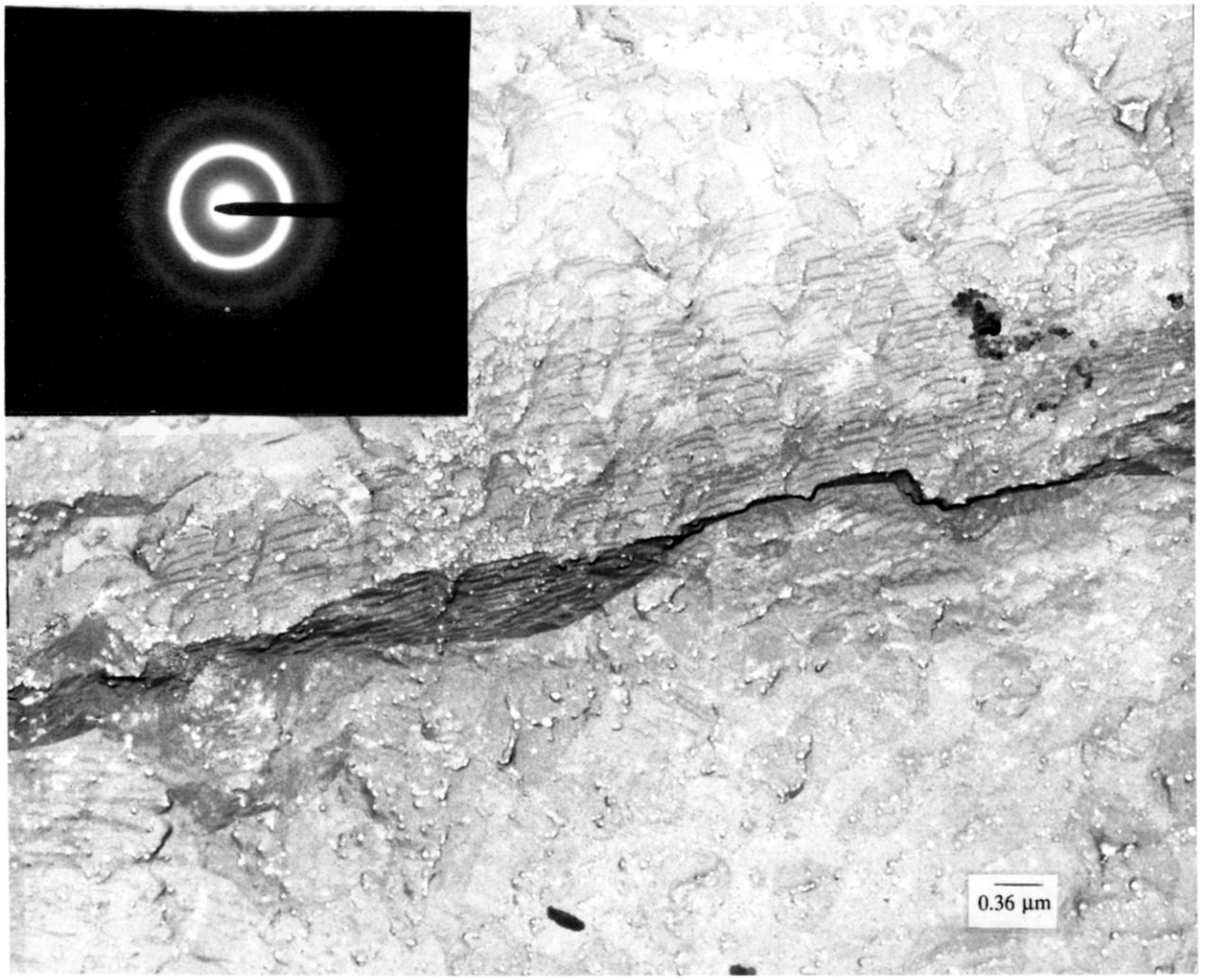

Figure 13. Bright-field TEM of high-phosphorus EN coating.

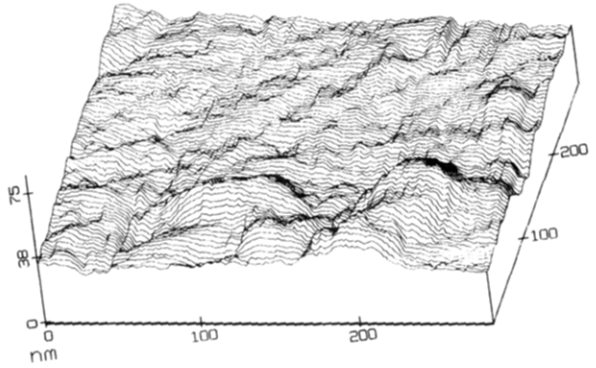

Figure 14. STM of high-phosphorus EN deposit showing smooth surface.

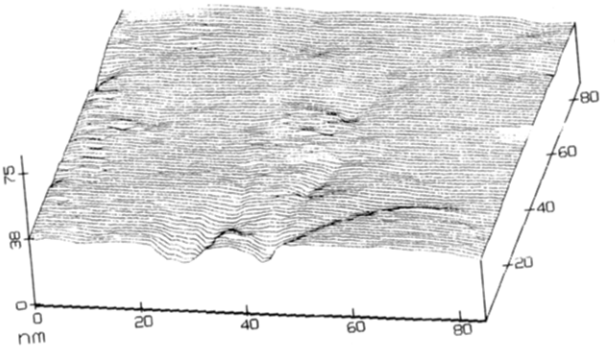

Figure 15. STM of high-phosphorus EN coating.

these deposits are completely amorphous. Dark-field imaging revealed no coherently diffracting crystallites.

STM analysis (Figure 14) shows a fairly smooth surface compared to the low- and medium-phosphorus deposits. Figures 15 and 16 show higher magnification images of Figure 14; large areas approximately 40 nm across are essentially featureless. Figure 16 shows very small surface features about 1–3 nm across.

A TEM image of a 50 nm thick chromium deposited on the polished copper foil is shown in Figure 17. The copper foil was removed prior to TEM analysis. The grains of chromium are the small black dots, approximately 10 nm and close to the size of the low-phosphorus nickel crystallites. The chromium deposit appears to grow epitaxially on the copper; the apparent twin in Figure 17 was originally present in the copper foil.

Discussion

The potential–pH coordinates (−0.295 V vs SCE, pH 6.8) of a copper electrode in the low-phosphorus solution lies close to the Cu_2O domain. However, at pH 4.7 and 4.8 metallic copper is the most thermodynamically stable species. It is possible the copper surface is covered by an oxide or hydrated hydroxide film in the low phosphorus electroless nickel solution. The lower pH of the medium- and high-phosphorus solution would tend to minimize oxide formation. The chelating present

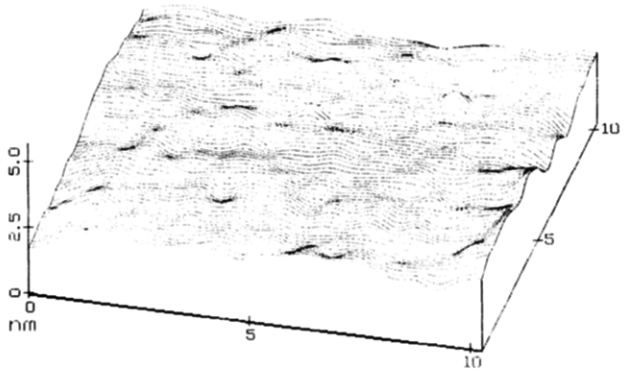

Figure 16. STM of high-phosphorus EN deposit showing TDS.

in the three electroless nickel solutions do not form stable compounds with copper.

Electroless nickel deposits from the low-, medium-, and high-phosphorus solutions did not copy the grain structure of the copper substrate. The growth of electrodeposited nickel on {100} copper has been studied by numerous authors because of the small misfit (3%) between nickel and copper. This small misfit between lattice parameters leads to epitaxial deposits of nickel on copper.[22-24] Itoh et al.[25] showed nickel deposits on (001) copper formed small isolated islands varying from several 10 to 100 nm in size. Similarly, Bicelli and Poli[26] showed nickel deposition onto various copper single crystals followed the structure of the base metal. Deposits on Cu(100) formed pyramids with square bases. The electroless nickel structures observed in this work are completely different than those deposited electrolytically on copper {100}. The composition and pH of the plating solutions have a strong influence on the resultant electroless nickel structure. Low-phosphorus electroless nickel films, 50 nm thick, are crystalline and discontinuous. Decreasing the pH of the nickel solutions results in an increase in occluded phosphorus in the nickel coating. Additions of carboxylic acids capable of dehydrogenating at a nickel electrode also facilitate phosphorus incorporation in the nickel deposits. Concomitant with the increase in occluded phosphorus is a decrease in the crystallinity of the nickel film. Various growth modes of electroless nickel on different surfaces have been observed.[27,28] The initial structure of EN deposits has been associated with different modes of activation of the substrate. Copper is not catalytically active toward the oxidation of $H_2PO_2^-$. An induction period prior to the deposition of nickel is often observed. In addition, copper is a noble metal reacting with oxygen and water more readily than Hg or Ag. Cu(I) and Cu(II) oxides would form, dependent upon pH, and would thus change the number of activation sites. A change in the density of active sites for electroless nickel nucleation changes the structure of the initial EN deposits. Marton and Schlesinger[27] showed the critical film thickness at which the EN deposit is continuous is dependent upon the density of active surface sites for nucleation. Cortijo and Schlesinger[28] showed that EN structures were also dependent upon the pH of the solution.

The composition of the electroless nickel solutions also has a strong influence on the degree of epitaxial growth of the nickel films. The fact that the grain structure of the copper substrate is not copied by the electroless nickel deposits yet replicated by electrolytic nickel deposits cannot be due to the fine-grained structure of the electroless nickel films. The structure of the copper {100} substrate was replicated by the chromium deposit, Figure 17. The grain structure originally present in the copper is present in the chromium foil. The large twin and bend fringes in Figure 17 were copied by the chromium. Dark-field analysis showed the grain size of the chromium deposit is approximately 10 nm and is in agreement with other reports for the crystallite size of chromium. Previous STM analysis of the chromium foil revealed the crystallites have a pyramidal shape about 3 nm wide. Therefore, the loss of substrate replication must be due in part to adsorbed species such as hypophosphite, organic acids, and stabilizers on the nickel surface.

STM images revealed three-dimensional structures (TDS) in all the deposits, the size of the TDS decreasing with increasing phosphorus content. It is difficult to determine if these TDS are deposited on an underlying continuous layer (e.g., Stranski–Krastanov mechanism) or if they form directly on the substrate (e.g., Volmer–Weber mechanism). The surface energy of nickel and copper is approximately 1700 and 1400 erg/cm^2, respectively.[29] This difference is probably too small to initiate complete Volmer–Weber type growth. It is likely this TDS prevailed because foreign substances were already adsorbed on the substrate.[18,19] Riedel.[30] showed the electrode surface during electroless nickel reduction is covered with adsorbed nickel and hypophosphite radicals. In addition, molecules such as propionic and tartaric acid are adsorbed and dehydrogenate on the nickel surface.[31] Thus, there are numerous adsorbed species which can affect the deposition process. The shape of the crystallites depends on adsorption of addition agents or products of their decomposition. Molecules which are incorporated in the deposit may completely stop the lateral spreading of a layer. Nucleation can occur only at discrete sites, and lateral spreading of the layers is impeded. Three-dimensional surface structure have been shown to develop[14] when the lateral spreading of atom rows is impeded so that a layer stops spreading as shown in Figures 10–12. When new layers are deposited on top of inhibited ones, they cannot overtake it. Thus a third dimension is created. The resultant structure is said to be bunched. The TDS shown in Figures 6, 10, and 16 possibly formed as a result of bunching due to adsorbed hydrogen, phosphorus, oxides of nickel, and/or stabilizers of other addition agents.

The deposit structure changed from a crystalline material in deposits containing less than 4 wt/wt % phosphorus to a semiamorphous structure in coatings

(22) Choi, H. J.; Weil, R. *Proc. Symp. Electrocryst.* **1981**, 169.
(23) Farr, J. P. G.; McNeil, A. J. S. *Proc. Symp. Electrocryst.* **1981**, 169.
(24) Farr, J. P. G.; McNeil, A. J. S. *Chem. Soc. Faraday Symp.* **1978** *12*, 145.
(25) Itoh, S.; Yamazoe, N.; Seiyama, T. *Surf. Technol.* **1977**, *5*, 27.
(26) Bicelli, L. P.; Poli, G. *Electrochim. Acta* **1966**, *11*, 289.
(27) Marton, J. P.; Schlesinger, M. *J. Electrochem. Soc.* **1968**, *115*, 16.
(28) Cortijo, R. O.; Schlesinger, M. *J. Electrochem. Soc.* **1983**, *130*, 2341.
(29) Zangwill, A., *Physics at Surfaces*; Cambridge University Press: Cambridge, Great Britain, 1989.
(30) Riedel, W. *Electroless Nickel Plating*; ASM International: Metals Park, OH, 1991.
(31) Mallory, G. O.; Hajdu, J. B. *Electroless Plating*; American Electroplaters and Surace Finishers Socety: Orlando, FL, 1990.

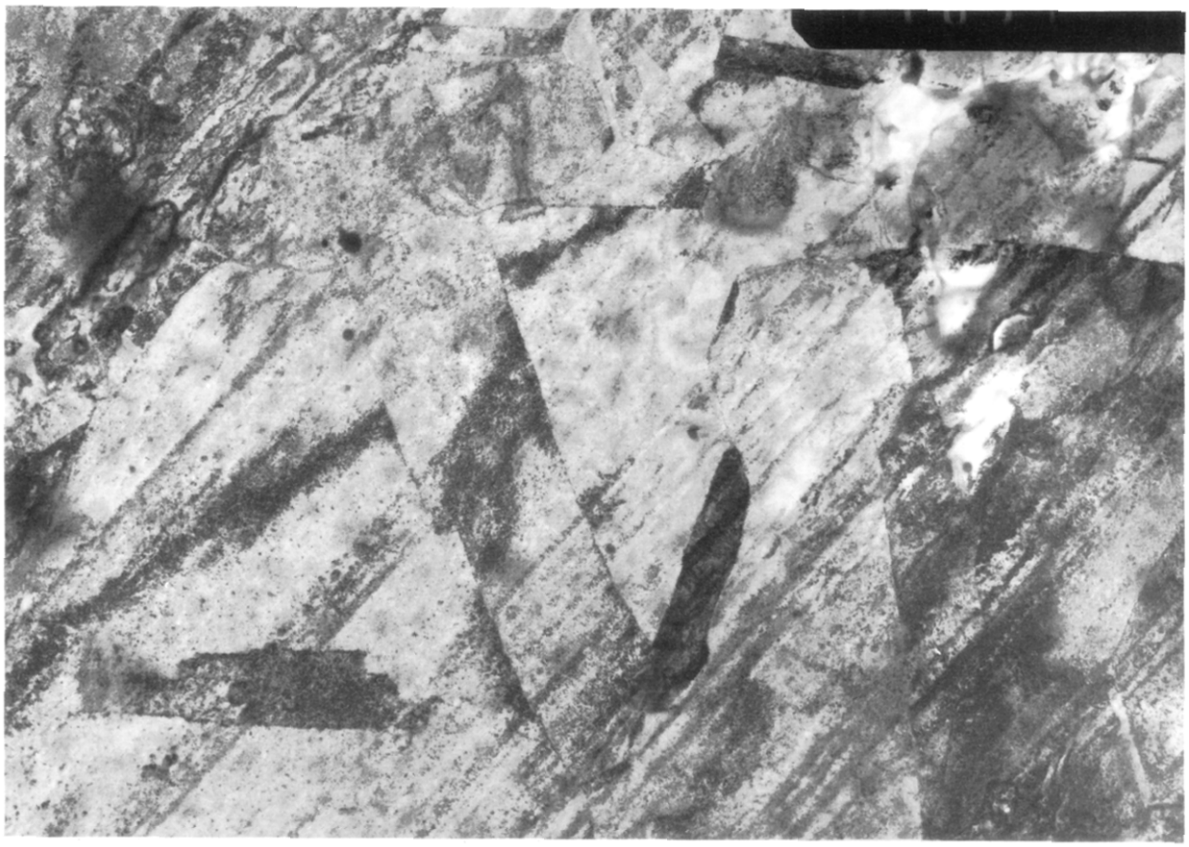

Figure 17. TEM of 50 nm thick chromium film showing grain structure of copper substrate.

between 5 and 8% phosphorus. Electron diffraction revealed an amorphous structure in deposits containing greater than 8% phosphorus. The incorporation of phosphorus in EN deposits is complex and not well understood.[30,31] Growth impediment due to foreign substances results in new grains being constantly nucleated. The result is a very fine-grained deposit. It is likely that either adsorbed hydrogen, phosphorus, or other reaction byproducts impeded growth, thereby causing nucleation of new grains. This repetitive nucleation caused the high phosphorus coatings to have the smallest crystallite size. The fine surface structures observed in Figures 6, 10, and 16 are similar in size to the coherently diffracting crystallites seen in the TEM images in Figures 3, 8, and 13, and this particle size agrees well with those previously calculated.[32,33]

Conclusion

The structures of EN coatings varying in occluded phosphorus were characterized using STM and TEM. STM studies revealed the third dimension of the TEM micrographs. The initial structure appears to be dependent upon the percent occluded phosphorus. EN deposits grow by the lateral spreading of atomic rows. TDSs probably result due to adsorbed species on the depositing surface. STM results on the size of the TDS correlates well with the size of the coherently diffracting crystallites from TEM studies. The size of the TDSs decreases with increasing phosphorus. The initial structures of low phosphorus deposits were island-like, whereas medium and high phosphorus deposits were more continuous.